Precipitation Dynamics for the Formation of Nylon-6 Polyamide Membranes by Isothermal Precipitation in Water/Formic Acid Solutions

Chien-Hsueh Shih[1], Carl C. Gryte[1] and Liao-Ping Cheng[2,3]*

[1]*Department of Chemical Engineering and Applied Chemistry, Columbia University, New York, NY 10027, U.S.A.*
[2]*Department of Chemical and Materials Engineering, Tamkang University, Tamsui, Taiwan, 251, R.O.C.*
[3]*Energy and Opto-Electronic Materials Research Center, Tamkang University, Tamsui, Taiwan, 251, R.O.C.*

Abstract

The ternary mass transfer equations that describe the isothermal immersion process for polyamide membrane preparation were solved. To account for the moving boundary conditions, coordinate transformations were performed both for the membrane and the bath regions. Mutual diffusion coefficients between solvent and polymer were measured and used to derive ternary phenomenological coefficients for mass transfer equations. The calculated precipitation times, concentration profiles, and diffusion trajectories were found to agree with the measured light transmittance data and the membrane morphologies presented previously.

Key Words: Nylon-6, Membrane, Ternary, Diffusion, Precipitation

1. Introduction

Microporous membranes of crystalline polymers are most often prepared by the immersion-precipitation method [1–12].The morphologies of Nylon-6 and Elvamide (a terpolymer of Nylon-6, -66 and -610) membranes formed by this method have been discussed previously [3]. Because Elvamide terpolymer is essentially amorphous, precipitation takes place exclusively in the form of liquid-liquid phase separation [11,12]. The formed membranes are asymmetric being composed of a dense nonporous skin layer and a mostly uniform supporting solid matrix. Unlike the terpolymer, Nylon-6 is crystalline and is therefore capable of precipitating from formic acid-water solutions either by liquid-liquid phase separation or by crystallization into cellular or particulate morphology, depending upon which of these two mechanisms is kinetically favored [11,12].

The dynamical circumstances after contact of the membrane solution with the coagulation bath was originally modeled as a ternary mass transfer problem by Cohen et al. [13]. Since then, various modifications (coordinate transformation, interaction parameters, diffusion coefficients etc.) by Reuvers [14,15], Tsay [16], Cheng [17] etc., were made to improve the accuracy of computation for the water-acetone-cellulose acetate system. All of these models assume that local equilibrium is established at the membrane-bath interface at the instant of immersion, and that phase separation occurs immediately after the binodal is entered by the diffusion trajectory. In fact, the most significant improvements to Cohen's model are the use of more accurate diffusion coefficients and the inclusion of the cross terms in the ternary diffusion equations. Using interferometry, Cheng et al. measured the mutual diffusion coefficients between solvent and polymer for moderately concentrated solu-

*Corresponding author. E-mail: lpcheng@mail.tku.edu.tw

tions [18]. These data were combined with Duda's theory to yield diffusivities over the applicable concentration range. Reuvers et al., on the other hand, derived diffusion coefficients from sedimentation data measured in dilute polymer solutions [15]. These diffusion data were also used by Tsay et al in their mass transfer model [16]. Numerical solutions of all of the above models were expressed in terms of the concentration profile of each component in the membrane solution as a function of time. The calculated results were found to agree with the morphology of the formed membranes (e.g., the thickness of the skin, the uniformity of the porous structure etc.). Smolders et al has categorized the phase separation process, using the precipitation onset times, into the instant demixing and the delayed demixing types [15]. The former case yields a membrane characterized by a thin skin and finger-like macrovoids whereas the later by a thick skin and various forms of cellular pores.

Cheng et al., analyzed the formation of Nylon-66 membranes by precipitation from formic acid aqueous solutions [11,12]. Depending upon the relative rate of crystallization and liquid-liquid phase separation, there are three typical situations often encountered: (1) Liquid-liquid phase separation precedes and dominates the precipitation process. The membrane is composed of cellular pores that are commonly observed in amorphous membranes, even though Nylon-66 is crystalline in nature. (2) Liquid-liquid phase separation and crystallization occur together during the course of precipitation. A membrane morphology mixed with cellular pores and crystalline particles is observed. (3) Crystallization initiates and dominates the precipitation process. The formed membrane is uniform and skinless, similar to the commercial Nylon-6 [19] and Nylon-66 [20] microporous membranes.

In contrast to Nylon-66, the melting point and thus the crystallization isotherm of Nylon-6 is significantly lower [21]. In this research, the mass transfer events during immersion precipitation for the formation of Nylon-6 membranes are investigated. Calculated results in terms of concentration profiles and diffusion trajectories of various preparation conditions are found to be consistent with the membrane morphology shown in part I of this series of papers.

2. Theory

The immersion precipitation process for preparing polyamide membranes is shown schematically in Figure 1, in which a thin layer of polymer solution cast on a flat surface is immersed in a large volume of bath liquid. Nonsolvent and solvent diffuse in opposite directions across the membrane-bath interface with fluxes J_1 and J_2, respectively. As the casting solution is transported through the bath with velocity v_∞, a hydrodynamic boundary layer, δ, and a concentration boundary layer, δ_c, are formed. Because fluxes J_1 and J_2 are generally different, the membrane-bath interface changes its position during the immersion precipitation process. This moving boundary problem is treated by a material coordinate transformation referenced to the polymer component [12,14]. Thus, the membrane-bath interface is always located at "zero" in this material coordinate. The inequality of sol-

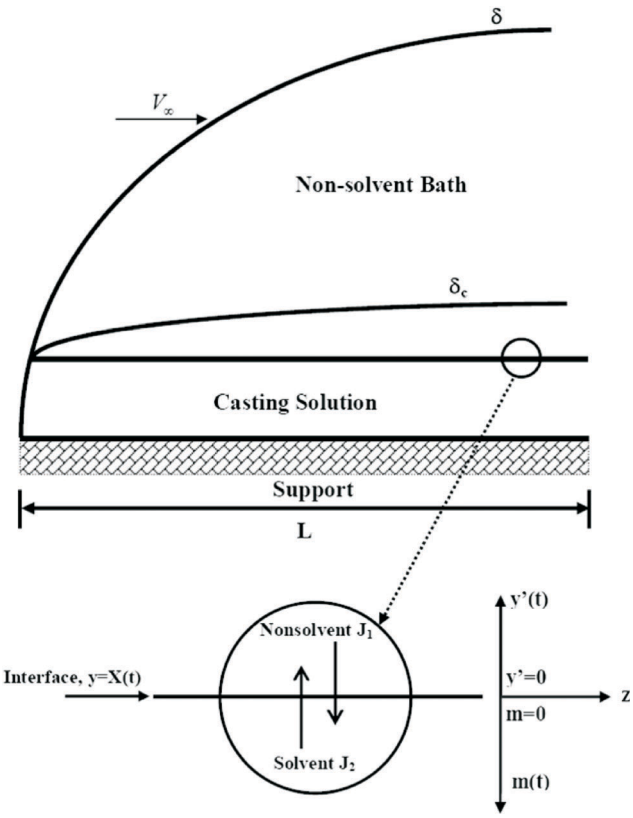

Figure 1. Schematic representation of the casting solution and the nonsolvent bath. δ and δ_c are the hydrodynamic and the concentration boundary layer respectively. V_∞ is the free stream velocity. m(t) is the material coordinate for the membrane solution. y′(t) is the coordinates for the nonsolvent bath.

vent and nonsolvent fluxes also results in the variation of interfacial compositions with time in the immersion process. Such effects has been discussed in several references [12,14–16]. The equation of continuity suited to the membrane solution region has been shown previously [12]:

$$\frac{\partial\left(\frac{\phi_1}{\phi_3}\right)}{\partial\tau}=\frac{V_1}{D_o}\frac{\partial\left(\phi_3 L_{11}\frac{\partial\mu_1}{\partial\eta}+\phi_3 L_{12}\frac{\partial\mu_2}{\partial\eta}\right)}{\partial\eta} \tag{1}$$

$$\frac{\partial\left(\frac{\phi_2}{\phi_3}\right)}{\partial\tau}=\frac{V_2}{D_o}\frac{\partial\left(\phi_3 L_{21}\frac{\partial\mu_1}{\partial\eta}+\phi_3 L_{22}\frac{\partial\mu_2}{\partial\eta}\right)}{\partial\eta} \tag{2}$$

where ϕ_i and V_i are the volume fraction and the partial molar volume of component i. In our notation, components 1, 2, and 3 are non-solvent, solvent, and polymer, respectively. μ_i is the chemical potential of species i. A modified Flory-Huggins expression for ternary system is used to compute μ_i in this work [12,21]. Eqs. (1) and (2) are transport equations expressed in dimensionless forms. The dimensionless time, τ, and the dimensionless distance, η, are defined as: $\tau = D_0\, t/M^2$ and $\eta = m/M$, where D_0 is the pre-exponential factor for the diffusion coefficient in Duda's expression [22]. M is the volume per unit area of the initial membrane solution before immersion. The polymer coordinate, m, as shown in Figure 1, is defined as the volume of polymer between the membrane-bath interface and the position of observation per unit area. L_{ij} $(i, j = 1, 2)$ are coefficients for the phenomenological expressions of diffusional fluxes with respect to the polymer component [12,23, 24]. According to Onsager's law, the cross coefficients must be equal, i.e., $L_{12} = L_{21}$ [23,24].

Since polymer is excluded from the bath, the equation of continuity for this region is identical to that for a binary system and is given in dimensionless form below[3,8]

$$\frac{\partial\phi_1}{\partial\tau}=\frac{M^2}{\delta_c^2}\frac{\partial\left(\frac{D_{12}}{D_o}\frac{\partial\phi_1}{\partial Y}\right)}{\partial Y}+\frac{1}{D_o}\left(-\frac{3}{8}\frac{V_\infty M^2\delta_c Y^2}{k\sqrt{z^3}}+\frac{3}{16}\frac{V_\infty M^2\delta_c^3 Y^4}{k^3\sqrt{z^5}}\right)\times\left(\frac{\partial\phi_1}{\partial Y}\right)(f+1) \tag{3}$$

The coordinate of the bath region, as shown in Figure 1, is selected such that the interface is always at y′ equal to zero (i.e., y′ = -y + X(t); X(t) is the position of the interface measured with respect to laboratory coordinate). In Eq. (3), the dimensionless distance, Y, is defined equal to y'/δ_c, where $\delta_c = \delta(D_{12}/\nu)^{1/3}$ is the thickness of the concentration boundary layer. $\delta = 4.64\ (\nu z/V_\infty)^{1/2}$ is the thickness of the hydrodynamics boundary layer. ν and D_{12} are the kinematic viscosity and the mutual diffusion coefficient for the bath liquid. V_∞ is the velocity of the free stream. k in Eq. (3) is equal to $4.64\ (\nu/V_\infty)^{1/2}$. f is a factor which accounts for the effect of mass transfer in the z direction [25]. Calculated results for the case of f = 0 are reported in this work.

The initial and boundary conditions are identical to those given in a previous publication [12]. Interfacial equilibrium is assumed to be established instantly after contact of the membrane solution with the bath. Hence, the interfacial compositions are always located at the binodal (i.e., ends of tie lines). Following Reuvers [14, 15], Dunlop's [26] method was employed to compute the phenomenological coefficients, L_{ij}, based on binary diffusion coefficients. The detailed procedure which involves the manipulation of binary and ternary friction coefficients are given in a precious publication [17]. The concentration dependent diffusion data for Nylon-6 and terpolymer in formic acid are measured by interferometric method and the results are shown elsewhere [18]. Only one non-experimental parameter, C, which relates the ternary friction coefficients R_{13} and R_{23} is used in this model. The effect of C on the calculated precipitation times are discussed in a previous paper [17].

3. Experimental and Computational Methods

3.1 Method for the Measurement of Precipitation Time

The optical system is shown in a previous publication [17]. A collimated light beam is passed through a series of filters, lens, and collimators. The beam is then directed towards the membrane solution. A glass cylinder is used to prevent the scattering caused by surface waves upon immersion. It also acts as a fine collimator. Using an optical fiber, the transmitted beam is guided to-

wards a monochromator, where the wave length corresponding to the optical filter is selected. This light signal is then transformed to an electrical signal and sent to the data acquisition system to give the light intensity of the transmitted beam. The experiment was carried out a 25 °C.

Dope solutions were prepared by mixing appropriate amounts of water, formic acid and Nylon-6 in glass bottles with Teflon lined cap at room temperature. The mixtures were then blended on a roll mill for 1-2 days to dissolve the polymer. The dope with high nonsolvent content was heated for 1 h. at 50 °C and then blended again at room temperature for another 12 h. to ensure complete dissolution. The fomed dope was cast on on a glass slide (4 cm × 6 cm), and then rapidly immersed into the nonsolvent bath [3]. The light transmittance was recorded with the data acquisition system and the intensity profiles were plotted. Examples of light transmission intensity as a function of time are given for different membranes and bath compositions in Figure 2. The time at which light intensity started to decrease was identified as the onset of observable precipitation (e.g., 22 s. for curve R in Figure 2) and the time at which light intensity fell to a constant minimum value was identified as the completion of precipitation (e.g., 55 s. for curve R in Figure 2). The data are found to be repeatable within about 20% deviation.

3.2 Computational Method

A computer program was written to perform the computations based on the finite difference method with 4^{th} order Runge-Kutta intergration. The casting solution was divided into 20 layers and the bath into 200 layers. For casting of a 25 vol% dope solution with casting thickness 250 μm, 20 layers correspond to a layer of ~3 μm with reference to the material coordinate, M. Claculations with larger number of layers (e.g., 30 and 40 layers) have been attempted, yet, not much improvement of the results is yielded. On the other hand, a simple calculation gives the concentration boundary layer of ~920 μm. If the bath is separated into 300 layers, then each layer will be ~3 μm, similar to the casting solution. However, actual calculation indicates that 200-layer is good enough to generate similar results. A local equilibrium was assumed to establish at the interface of the casting solution and the bath immediately after their contact. The input parameters for model computation can be found in Table 1 of reference [12], except for the molecular weight and molar volume of Nylon-6, which are M = 59,000 g/mol and V_3 = 32,000 cm^3/mol, respectively. Interaction parameters and binary mutual diffusion coefficient, D_{23}, were taken from literature [18]. Various situations corresponding to different preparation conditions were calculated. The calculated concentration distribution was combined with the equilibrium phase diagram to yield diffusion trajectories that were subsequently used to show the formation mechanism of membrane morphologies discussed previously.

4. Results and Discussion

Measurements of precipitation times and calculations of diffusion paths were performed for different dope compositions. The rate of precipitation for these cases was measured by the optical method described previously. The dopes contained approximately 23.5 vol% polymer and increasing amounts of water (cf. Figure 8 of reference [3]).

4.1 Immersion of a Low Water Dope in a Soft Bath

In Figure 3, calculated trajectories are given for the case of immersing dope A containing almost no water

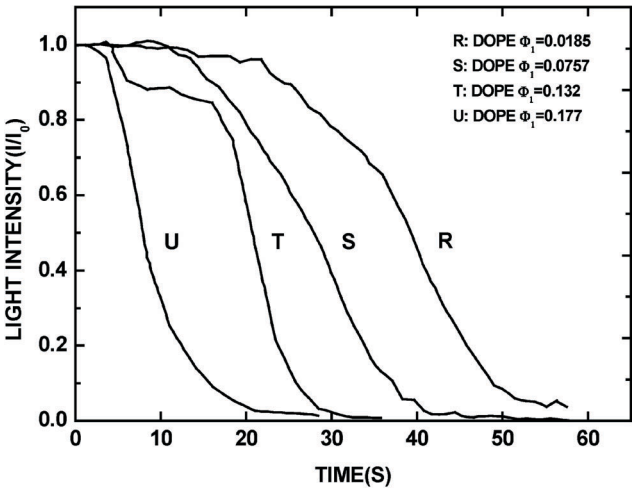

Figure 2. Light transmittance during immersion of Nylon-6 casting solutions into a water bath. Dope compositions: R (ϕ_1 = 0.018, ϕ_3 = 0.239), S(ϕ_1 = 0.0757, ϕ_3 = 0.237), T(ϕ_1 = 0.132, ϕ_3 = 0.234), U(ϕ_1 = 0.177, ϕ_3 = 0.232).

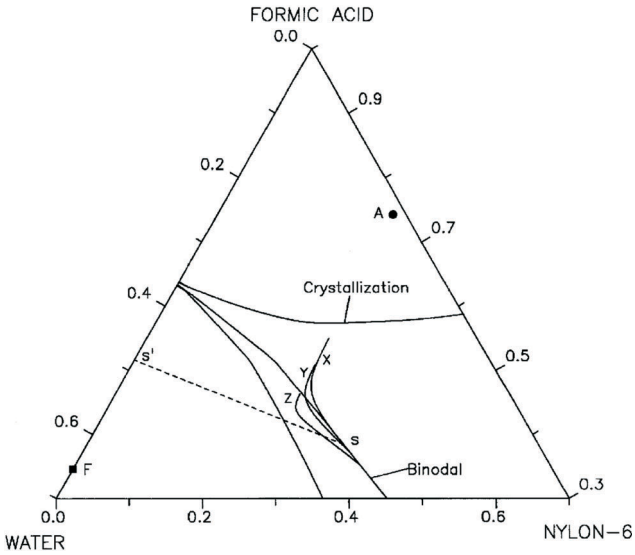

Figure 3. Calculated diffusion trajectories for the water-formic acid-polyamide system. Composition of dope A: $\phi_1 = 0.021$, $\phi_3 = 0.239$. Bath F: 39.2 wt.% formic acid in water. Line ss′: equilibrium tie line. Trajectories: X at 51.3 s.; Y at 65.6 s.; Z at 99.8 s.

into a 39.2 wt.% formic acid aqueous solution (bath F). This bath is very soft and precipitation in this bath is a relatively slow process. Trajectories X, Y, and Z represent, respectively, the local compositions within the casting solution at 51 s., 66 s., and 100 s. after contact of the dope with the bath. For each trajectory, the composition of the membrane-bath interface is located at the binodal, consistent with the assumption of an equilibrium boundary condition. For example, point 'S' on trajectory X represents the composition at the interface of membrane solution that is in equilibrium with the interfacial composition of bath represented by point 'S′'. The bottom surface of the membrane solution is located at the other end of the trajectory. Trajectory X shows that, at 51 s. after immersion, the top layer of the casting solution begins to cross the binodal phase boundary into the region where both liquid-liquid phase separation and crystallization are possible. Although this computed phase separation time is somewhat longer than the measured 42 s. onset time for precipitation, it is considered within the experimental error and its effect will be discussed later. Examining the morphology of the membrane prepared in this condition (Figure 10(a) of reference [3]) revealed a liquid-liquid phase separation dominated morphology. Nucleation of polymer crystal was slow because it required the deprotonation of all hydrogen-bonded amide group of the Nylon-6 polymer that was dissolved in a good solvent, formic acid. By contrast, nucleation of liquid micells by liquid-liquid phase separation was easier and hence, it took place shortly after the membrane solution became supersaturated with respect to liquid-liquid phase separation.

Although phase separation might commenc after the binodal was crossed, the trajectory calculation has been performed beyond the time when binodal miscibility envelop was entered (e.g., 51 s. in this case). In other words, it has been assumed that significant precipitation has not yet begun. As more and more solvent and non-solvent diffused across the membrane-bath interface, an increasingly larger part of the trajectory fell within the binodal region (e.g., trajectory Y). At 101 s. after immersion, as shown by trajectory Z, the whole membrane solution has crossed the binodal. If crystallization was precluded, precipitation by liquid-liquid phase separation process was expected to occur over the entire membrane cross section. In Figure 4, the polymer volume fractions (ϕ_3) corresponding to trajectories X, Y, and Z in Figure 3 are plotted as a function of the depth into the membrane solution, y. In each concentration profile, the point at y = 0 represents the membrane-bath interface

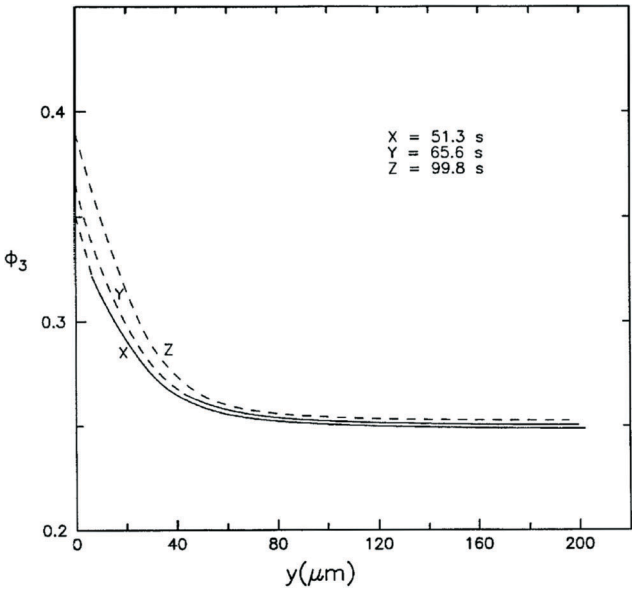

Figure 4. Calculated polymer volume fraction profiles as a function of distance for dope A into bath F. X at 51.3 s., Y at 65.6 s., and Z at 99.8 s. y = 0 denotes the membrane-bath interface.

and the other end point represents the bottom surface of the membrane solution. The dotted portion of each curve stands for the region inside the binodal envelop whereas the solid part of each curve is the region outside the binodal envelop. Figure 4 indicates that most of the membrane solution remains essentially at a constant polymer volume fraction (ϕ_3~0.25) for the period of at least 100 s. Since phase transformation occurs within this time frame, a uniform porous morphology is anticipated for the cross section of the final membrane. The increased polymer volume fraction near the interface is relevant to the observed skin region near the membrane top surface. As shown in Figure 4, the interfacial polymer concentration reaches ca. 36 vol.% when phase separation starts and it increases continuously throughout the precipitation process. These high polymer concentrations can retard the formation of liquid micells by liquid-liquid phase separation in this region. On the other hand, the top surface is highly supersaturated with respect to crystallization. Nucleation of polymer crystal occurs just underneath the interface and grow following the habit of two dimensional spherulites into the observed polygonal plate structure (cf. Figure 11(a) of reference [3]).

4.2 The Effect of Water Content in the Dopes

In Figure 5, measured precipitation times for immersing dopes containing increasing amount of water into bath F are given for Nylon-6 (square points) and for a structurally similar polyamide terpolymer, Elvamide (round points). Because this terpolymer cannot crystallize to any significant degree, it is to be expected that precipitation does not occur until the binodal is crossed. Therefore, the onset of precipitation for the terpolymer is considered to be nucleation and growth of liquid micells resulted from liquid-liquid phase separation. Nylon-6, unlike the terpolymer, may initially precipitate by crystallization, liquid-liquid phase separation, or a simultaneous precipitation of both types. As shown in Figure 5, for both polymers, increasing water content in the dope always reduces the precipitation time, and as water content is increased to ca. 24 vol.% (dope D), an instantaneous initiation of precipitation is observed. In such a high water-content dope, the polymer is poorly solvated and precipitation occurs upon slight concentration fluctuation, as soon as nonsolvent is transported into the membrane solution. The measured induction times for initiation of precipitation (solid symbols, ■ and ●) for Nylon-6 and terpolymers are similar in all dope conditions. It takes, however, ca. 20~30 seconds longer for Nylon-6 to completely precipitate (open symbols, □ and ○) than the terpolymer.

Because the interaction parameters and the diffusivities are almost the same for both polymers, trajectory calculations for Nylon-6 and the amorphous terpolymer yield very similar results. The calculated precipitation times common to terpolymer and Nylon-6 are shown in Figure 5. The dashed lines represent the calculated times for crossing binodal by the first, 5th, and 20th (bottom) layers of the membrane solution. The measured time for complete precipitation of the terpolymer membrane solution is roughly consistent with the computed time required for the 20th layer (i.e. the whole membrane solution) to cross the binodal. This calculation ignores the effect of precipitation on the rate of mass transfer.

In Figure 6, calculated compositions of polymer

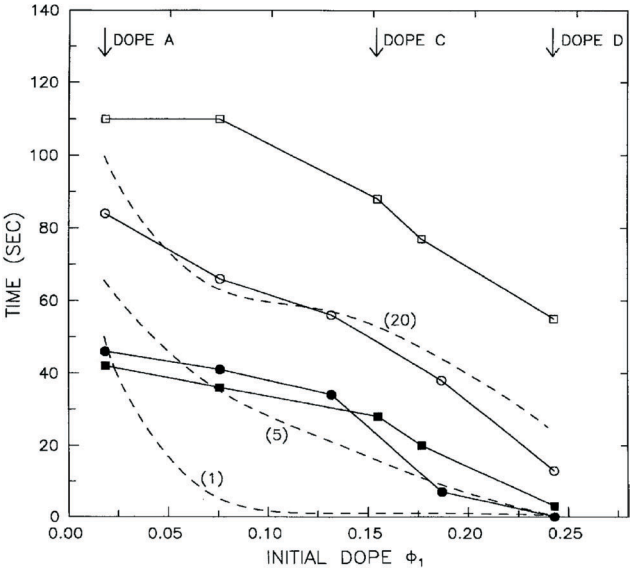

Figure 5. Measured (solid lines) and calculated (dashed lines) precipitation times for various polyamide dopes (ϕ_3~0.235) in bath F. ●, ■: onset precipitation times for terpolymer and Nylon-6, respectively. ○, □: end of precipitation as found from light transmission for terpolymer and Nylon-6, respectively. (1), (5), and (20) indicate calculated times for the first, fifth and last layer of casting solution to cross the binodal.

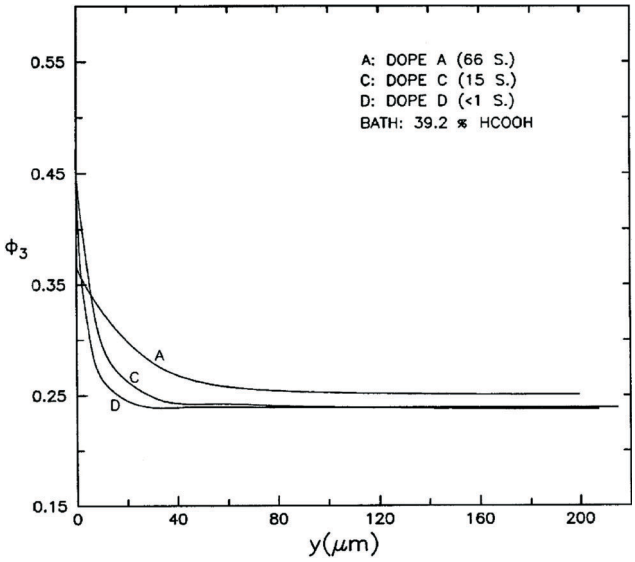

Figure 6. Calculated polymer volume fraction profiles as a function of distance when the 5th layer crosses the binodal for dopes A, C and D into bath F. y = 0 denotes the membrane-bath interface.

along the depth into the membrane solution at the time scale of phase separation (i.e.; the 5th layer cross the binodal) are compared for various dope conditions. Curves A, C, and D represent the cases where dopes A, C, and D were immersed in bath F, respectively. Curve A has been shown in Figure 4 (curve Y) and is redrawn here for comparison. Curve C shows that polymer concentration remains largely constant, close to the initial dope (ϕ_3~0.24), for most part of the casting solution, while at the interface, it reaches 43%. This implies that substantial mass exchange has occurred only near the interfacial zone when phase separation commences. This zone will act as a mass transfer barrier. Thus, curve C anticipates a uniform porous structure in the interior of the final membrane. This is consistent with the morphology of Nylon-6 membrane shown previously (cf. Figure 10(b) of reference [3]). In this SEM photomicrograph, a structure composed of open cellular pores surrounded by high population of crystallites is observed. Such a structure suggests that liquid-liquid phase separation and crystallization occurs concurrently during the course of precipitation. Since dope C is close in concentration to the crystallization line, nucleation of Nylon-6 crystals is expected to be more rapid than dope A which is in a well solvated state in formic acid. The top surface of this membrane is shown in Figure 11(b) of reference [3]. It is composed of independent polygonal spherulites that make this surface skinless. Formation of such structure is associated with the concentration of polymer near the interface. Instantly after contact with a bath, the interfacial polymer composition increases in a manner restricted by the equilibrium boundary condition. At the time for phase separation, curve C shows that interfacial volume fraction of polymer is about 43%. Thus, this top layer is essentially a soft gel highly supersaturated with respect to polymer crystallization. Nucleation within this layer occurs with each nucleus formed surrounded by a polymer-poor boundary. Since the nucleation density is quite high, all fully developed spherulites are separated, making the top surface of this membrane appear virtually skinless. The flattened appearance is a result of crystal growth against a planar interface.

Curve D in Figure 6 represents the case of a high-water dope immersed in a soft bath at the time of precipitation. Although dope D appears to be a clear solution, it is, in fact, on the edge of precipitation. This dope turns cloudy and then becomes a white gel upon standing at room temperature for 24 h. Upon immersion a fresh dope into a soft bath, precipitation occurs rapidly and crystallization is observed to dominate the formed morphology. The SEM photomicrographs (cf. Figures 10(c) and (d) of reference [3]) indicate that this Nylon-6 membrane has a largely uniform microporous structure composed of interlocked network of crystallites in the shape of sticks. It can also be seen sporadically small residues of cellular pores formed by liquid-liquid phase separation. Because this Nylon-6 dope solution is at a point of incipient crystallization, it contains a high population of subcritical crystal embryos. Any increase in nonsolvent by exchange with the bath results in an immediate nucleation of crystalline particles.

Curve D shows that in the very thin region (ca. 1% of the membrane solution) near the top surface, the polymer concentration reaches approximately 50% at the time of precipitation. This provides a favorable environment for nucleation of polymer crystal in the sense that this thin gel layer is in a high degree of supersaturation and is not mechanically robust. Polymer crystallization in this region, breaks up easily the thin and weak boundary gel

layer and eliminates any evidence of this layer in the final precipitation product. The outcome is a discontinuous porous top surface as shown in the SEM given in Figures 11(c) of reference [3].

Uniform skinless Nylon-6 microporous membranes can only be made when the dope solution is near the point of precipitation and the bath is soft. The presence of nonsolvent in the dope makes the polymer coils collapse on themselves as it does just prior to crystallization. Under such conditions, the driving force for dissolution is very small and thus these dope solutions have a "memory". Aggregation of the polyamide by hydrogen bonding and incomplete dissolution in the dope of the polymeric component may significantly alter the population of the subcritical embryo structures. As a result, the history of these solutions may dramatically affect particle density in the precipitated membrane. Since the "structure" that exists in these dopes is ordinarily very difficult to quantify, it is critical that very reproducible procedures be used to make these solutions if reproducible membrane structure is being sought. The soft bath, containing a high concentration of solvent has two purposes. First, due to the high solvent content, the driving force in the dope solution for mass transfer to cross the binodal is small and composition changes are relatively slow. This suppresses any tendency for liquid-liquid phase separation. Second, there is no significant tendency to form a thick, viscous, and dense impermeable skin layer at the membrane interface.

5. Conclusion

Crystalline Nylon-6 may be precipitated into a variety of morphologies from formic acid by contact with an aqueous nonsolvent bath. During this immersion process, the kinetical event that take places prior to phase separation (either initiated by liquid-liquid demixing or crystallization) is modeled as a mass transfer process in a ternary system. Computations are carried out for various dope conditions and the calculated results are incorporated with the phase diagram to yield diffusion trajectories. These trajectories indicate clearly the time frame and the manner membrane solutions enter the binodal and crystallization zones. Since both forms of precipitation are likely to happen, the formed membranes exhibit structures mixed with different degree of cellular pores and crystalline particles, depending upon the sequence of the precipitation processes and the nucleation density. The whole immersion precipitation process is followed optically and the onset and completion times validate the computed times for crossing the phase envelops. For dopes immersing in a soft bath, calculated concentration profiles points out the formation of a thin soft gel near the top surface and a constant concentration distribution along the bulk. This is consistent with the observed discontinuous top surface and a uniform membrane cross-section for various dopes.

Nomenclature

D_0	pre-exponential factor for the diffusion coefficient in Duda's expression
D_{12}	mutual diffusion coefficient
f	factor accounting for the effect of mass transfer in the z direction
J_1	diffusion flux of nonsolvent
J_2	diffusion flux of solvent
k	parameter defined in Eqn. (3), equal to 4.64 $(\nu/V_\infty)^{1/2}$
L_{ij}	phenomenological coefficients for diffusional fluxes ($i, j = 1, 2$)
M	volume per unit area of the initial membrane solution
m	polymer coordinate
V_i	partial molar volume of component i
v_∞	velocity of casting solution in the bath
X(t)	position of the interface measured with respect to laboratory coordinate
Y	dimensionless distance, y'/δ_c
y'	coordinate of the bath region, as shown in Figure 1, $y' = -y + X(t)$
δ	thickness of the hydrodynamic boundary layer
δ_c	thickness of the concentration boundary layer
η	dimensionless distance, $\eta = m/M$
ϕ_i	volume fraction of component i
μ_i	chemical potential of component i
τ	dimensionless time, $\tau = D_0 t/M^2$
ν	kinematic viscosity of the bath liquid

References

[1] Lin, D. J., Chang, C. L., Chen, T. C. and Cheng, L. P., "On the Structure of Porous Poly(Vinylidene Fluoride) Membrane Prepared by Phase Inversion from Water-NMP-PVDF System," *Tamkang Journal of Science and Engineering*, Vol. 5, pp. 95–98 (2002).

[2] Young, T. H., Chang, H. H., Lin, D. J. and Cheng, L. P., "Surface Modification of Microporous PVDF Membranes for Neuron Culture," *Journal of Membrane Science*, Vol. 350, pp. 32–41 (2010).

[3] Shih, C. H., Gryte, C. C. and Cheng, L. P., "Morphology of Membranes Formed by Isothermal Precipitation of Polyamide Solutions from Water/Formic Acid Systems," *Journal of Applied Polymer Science*, Vol. 96, pp. 944–960 (2005).

[4] Young, T. H., Lu, J. N., Lin, D. J., Chang, C. L., Chang, H. H. and Cheng, L. P., "Immobilization of l-Lysine on Dense and Porous Poly(Vinylidene Fluoride) Surfaces for Neuron Culture," *Desalination*, Vol. 234, pp. 131–143 (2008).

[5] Lin, K. Y., Wang, D. M. and Lai, J. Y., "Nonsolvent-Induced Gelation and Its Effect on Membrane Morphology," *Macromolecules*, Vol. 35, pp. 6697–6706 (2002).

[6] Zhao, Y. H., Zhu, B. K., Ma, X. T. and Xu, Y. Y., "Porous Membranes Modified by Hyperbranched Polymers: I. Preparation and Characterization of PVDF Membrane Using Hyperbranched Polyglycerol as Additive," *Journal of Membrane Science*, Vol. 290, pp. 222–229 (2007).

[7] Wang. X., Zhang, L., Sun, D., An, Q. and Chen, H., "Effect of Coagulation Bath Temperature on Formation Mechanism of Poly(Vinylidene Fluoride) Membrane," *Journal of Applied Polymer Science*, Vol. 110, pp. 1656–1663 (2008).

[8] Yeow, L. M., Liu, Y. T. and Li, K. "Morphological Study of Poly(Vinylidene Fluoride) Asymmetric Membranes: Effects of the Solvent, Additive, and Dope Temperature," *Journal of Applied Polymer Science*, Vol. 92, pp. 1782–1789 (2004).

[9] Blanco, J. F., Sublet, J., Nguyen, Q. T. and Schaetzel, P., "Formation and Morphology Studies of Different Polysulfones-Based Membranes Made by Wet Phase Inversion Process," *Journal of Membrane Science*, Vol. 283, pp. 27–37 (2006).

[10] Khayet, M., Mengual, J. I. and Mastsuura, T., "Porous Hydrophobic/Hydrophilic Composite Membranes: Application in Desalination Using Direct Contact Membrane Distillation," *Journal of Membrane Science*, Vol. 252, pp. 101–113 (2005).

[11] Cheng, L. P., Dwan, A. H. and Gryte, C. C., "Membrane Formation by Isothermal Precipitation in Polyamide-Formic Acid-Water Systems I. Description of Membrane Morphology," *Journal of Polymer Science, Polymer Physics*, Vol. 33, pp. 211–222 (1995).

[12] Cheng, L. P., Dwan, A. H. and Gryte, C. C., "Membrane Formation by Isothermal Precipitation in Polyamide-Formic Acid-Water Systems II. Precipitation Dynamics," *Journal of Polymer Science, Polymer Physics*, Vol. 33, pp. 223–235 (1995).

[13] Cohen, C., Tanny, G. B. and Prager, S., "Diffusion-Controlled Formation of Porous Structures in Ternary Polymer Systems," *Journal of Polymer Science, Polymer Physics*, Vol. 17, pp. 477–489 (1979).

[14] Reuvers, A. J., van den Berg, J. W. A. and Smolders, C. A., "Formation of Membranes by Means of Immersion Precipitation: Part I. A Model to Describe Mass Transfer during Immersion Precipitation," *Journal of Membrane Science*, Vol. 34, pp. 45–65 (1987).

[15] Reuvers, A. J. and Smolders, C. A., "Formation of Membranes by Means of Immersion Precipitation: Part II. the Mechanism of Formation of Membranes Prepared from the System Cellulose Acetate-Acetone-Water," *Journal of Membrane Science*, Vol. 34, pp. 67–86 (1987).

[16] Tsay, C. S. and McHugh, A. J., "Mass Transfer Modeling of Asymmetric Membrane Formation by Phase Inversion," *Journal of Polymer Science, Polymer Physics*, Vol. 28, pp. 1327–1365 (1990).

[17] Cheng, L. P., Soh, Y. S., Dwan, A. H. and Gryte, C. C., "An Improved Model for Mass Transfer during the Formation of Polymeric Membranes by the Immersion-Precipitation Process," *Journal of Polymer Science, Polymer Physics*, Vol. 32, pp. 1413–1425 (1994).

[18] Cheng, L. P., Dwan, A. H. and Gryte, C. C., "Measurements of Mutual Diffusivities in Concentrated Solutions of Membrane-Forming Polyamides and Cellu-

lose Acetate," *Journal of Applied Polymer Science*, Vol. 57, pp. 563–572 (1995).

[19] Marinaccio, P. J. and Knight, R. A., U.S. Patent 3,876,738 (1975).

[20] Pall, D. B., U. S. Patent 4,340,479 (1982).

[21] Cheng, L. P., Dwan, A. H. and Gryte, C. C., "Isothermal Phase Behavior of Nylon-6, -66, and -610 Polyamides in Formic Acid-Water Systems," *Journal of Polymer Science, Polymer Physics*, Vol. 32, pp. 1183–1190 (1994).

[22] Duda, J. L., Vrentas, J. S., Ju, S. T. and Liu, H. T., "Prediction of Diffusion Coefficients for Polymer-Solvent Systems," *AIChE Journal*, Vol. 28, pp. 279–285 (1982).

[23] Haase, R., *Thermodynamics of Irreversible Process*, Addison-Wesley, MA (1969).

[24] Fitts, D. D., *Nonequilibrium Thermodynamics*, McGraw-Hill, New York (1962).

[25] Cheng, L. P., *Mechanism of Microporous Membrane Formation by Precipitation of Semicrystalline Polymers*, Ph. D. Dissertation, Columbia University, New York, U.S.A. (1993).

[26] Dunlop, P. J., "Frictional Coefficients for Binary and Ternary Isothermal Diffusion," *Journal of Physical Chemistry*, Vol. 68, pp. 26–30 (1964).

Manuscript Received: Oct. 24, 2011
Accepted: Mar. 7, 2012